Limnol. Oceanogr., 55(2), 2010, 615–627

Simultaneous measurements of nitrate, oxygen, and carbon dioxide on oceanographic moorings: Observing the Redfield ratio in real time

Kenneth S. Johnson*

Monterey Bay Aquarium Research Institute, Moss Landing, California

Abstract

Autonomous observations of dissolved nitrate, oxygen, and total inorganic carbon (TCO_2, which is derived from pCO_2 and estimates of alkalinity) from sensors on the M1 and M2 moorings, off Monterey Bay, California, are examined. These observations are used to assess the linkages between nitrogen, oxygen, and carbon cycling with the Redfield ratio as a framework for the analysis. Concentrations of TCO_2, oxygen, and nitrate were high-pass filtered to remove low-frequency signals driven by water mass changes. Daily cycles in each property are apparent with maxima or minima at the end of daylight. These daily cycles are consistent with biological production of oxygen or uptake of TCO_2 and nitrate. Ratios of the changes in these diel cycles approach values expected from the Redfield ratio early in upwelling cycles. However, periods are frequently seen where the utilization of nitrate N is substantially lower than expected when compared to observed changes in TCO_2 or oxygen. During these periods, fixed nitrogen must be supplied from other sources, such as ammonium or urea, or it is obtained from deeper waters by vertically migrating phytoplankton. These migrating phytoplankton must then return to the surface where inorganic carbon is consumed and oxygen is produced.

Redfield (1934) observed that the concentrations of dissolved nitrate, oxygen, and inorganic carbon are present in the water and in plankton in nearly constant proportions. This observation has evolved toward an understanding that, on average, production or respiration of organic matter in the sea approximates the following equation:

$$106\ CO_2 + 16\ HNO_3 + 1\ H_3PO_4 + 122\ H_2O \leftrightarrow (CH_2O)_{106}\ (NH_3)_{16}\ H_3PO_4 + 138\ O_2 \quad (1)$$

The stoichiometric ratio $106C:16N:1P:-138O_2$ is termed the Redfield ratio. This concept of closely linked elemental ratios in the biogeochemical cycles of the ocean has served as one of the foundations of biogeochemical research in the nearly 75 yr since Redfield presented the concept (Falkowski 2000). The oceanographic community has expanded on these concepts primarily by collecting samples in surveys that now span the global ocean and then measuring concentrations in these samples on board ship or onshore to examine the processes that regulate marine biogeochemistry. These results generally confirm the Redfield assessment but have also led to revisions. For example, Anderson (1995) suggested that the oxygen coefficient be revised from −138 to −150. It is also clear that even the revised elemental ratios are not fixed, and abundant information on elemental cycling can be derived from anomalies relative to the mean values of the Redfield ratio. Spatial variability in elemental ratios has been reported by Anderson and Sarmiento (1994) and Li and Peng (2002). Details of the spatial variability in nutrient ratios have been used to estimate the global distribution of anthropogenic carbon (Gruber and Sarmiento 1997), nitrogen fixation (Deutsch et al. 2007), denitrification (Tyrell and Lucas 2002), and ocean mixing (Broecker 1974). There have been fewer studies of the variations in elemental ratios in time. Temporal changes on decadal scale in the elemental ratios found near the euphotic zone (Karl et al. 2001) and in deep waters (Pahlow and Riebesell 2000) have been discussed. Decadal scale changes in the Redfield ratio are, however, difficult to detect, particularly in deep water, because of the long residence times of the chemicals (Keller et al. 2002). Seasonal changes in C : N ratios have been noted in the North Atlantic, which appear to reflect overconsumption of N during rapid growth (Kortzinger et al. 2001). Although the community has gained greater insights into elemental cycling by using the Redfield ratio, the processes that create the near constancy in elemental ratios continue to be examined (Lenton and Watson 2000; Klausmeier et al. 2004).

It is now possible to measure nitrate (Johnson and Coletti 2002; Johnson et al. 2006; Kortzinger et al. 2008*b*), oxygen (Tengberg et al. 2006; Kortzinger et al. 2008*a*), and pCO2 (Friederich et al. 2002; DeGrandpre et al. 2006; Kortzinger et al. 2008*b*) on oceanographic moorings for near yearlong periods of time without substantial degradation in sensor performance. Each of these chemicals is closely linked through Eq. 1 to the primary production and respiration of organic carbon. For example, it has been demonstrated that diel cycles in concentration of nitrate can be used to provide near-daily estimates of primary production for sustained (years) periods (Johnson et al. 2006). Diel variations in oxygen and inorganic carbon are also used to examine temporal changes in primary productivity (Odum 1956; Yates et al. 2007). The capacity for long-term, autonomous observations of multiple chemicals now allows the linkages between chemical cycles to be monitored continuously (Johnson et al. 2007).

Here, I examine measurements of nitrate, oxygen, and inorganic carbon that were reported by in situ sensors on the M1 and M2 moorings offshore of Monterey Bay, California. These are highly instrumented moorings (Cha-

* Corresponding author: johnson@mbari.org

vez et al. 1997) that have been maintained since 1989. Measurements of ΔpCO_2, the difference in sea and air pCO_2, have been made since 1993 on these moorings (Friederich et al. 1995). These measurements have been used to examine long-term changes in air–sea gas exchange of CO_2 driven by processes such as El Niño (Friederich et al. 2002). Measurements of nitrate concentration on the moorings began in 2002 using optical nitrate sensors (Johnson and Coletti 2002). These measurements have been used to examine daily to annual changes in primary production (Johnson et al. 2006). Dissolved oxygen measurements using Aanderaa Optode sensors (Tengberg et al. 2006) became operational on both moorings in April 2006. This article uses the Redfield model as a framework to interpret the daily variations in the ratios of total dissolved inorganic carbon (TCO_2), whose concentration is calculated from pCO_2 and estimated titration alkalinity, dissolved oxygen, and nitrate. The analysis focuses on the period from April 2006 through August 2006. However, all these measurements continue, with some interruptions, through the present. The data are delivered to the Internet at several Web pages located at http://www.mbari.org, where they are available for analysis by the community.

Methods

The M1 and M2 mooring locations are 36.747°N, 122.022°W (1200-m depth) and 36.697°N, 122.378°W (1800-m depth), offshore of Monterey Bay (Fig. 1). These moorings are 20 and 50 km offshore, respectively. In addition, some data collected at the MSE mooring are shown. It was located at 36.2°N, 122.9°W (3300-m depth), which is 115 km offshore.

Nitrate was measured at 1-m depth using In Situ Ultraviolet Spectrophotometer (ISUS) nitrate sensors (Johnson and Coletti 2002). The mooring data, including the complete ultraviolet (UV) spectrum measured by ISUS, are transmitted to shore hourly. Nitrate concentrations are calculated using the measured light absorption spectrum from 217 to 240 nm and a linear baseline estimate. Biofouling of the optics was inhibited with a copper and Nitex antifouling shield. The ISUS sensor calculates nitrate concentration using the algorithm described in Johnson and Coletti (2002). A revised algorithm that substantially improves the accuracy of UV nitrate measurements has been developed (Sakamoto et al. 2009). All the data reported here were reprocessed from the observed ultraviolet spectra, temperature, and salinity with that new algorithm. This involves correcting the bromide molar absorptivities to the in situ temperature. The salinity measured with the conductivity, temperature, and depth (CTD) sensor is then used to predict bromide ion concentration using the known bromide-to-chlorinity ratio (Morris and Riley 1966), and the temperature-corrected bromide molar absorptivities are used to calculate the UV spectrum due to bromide. This bromide spectrum is subtracted from the observed UV spectrum. Nitrate is determined by fitting the bromide corrected sea water spectra with the molar absorptivities of nitrate, which are temperature independent, and an absorbance baseline that

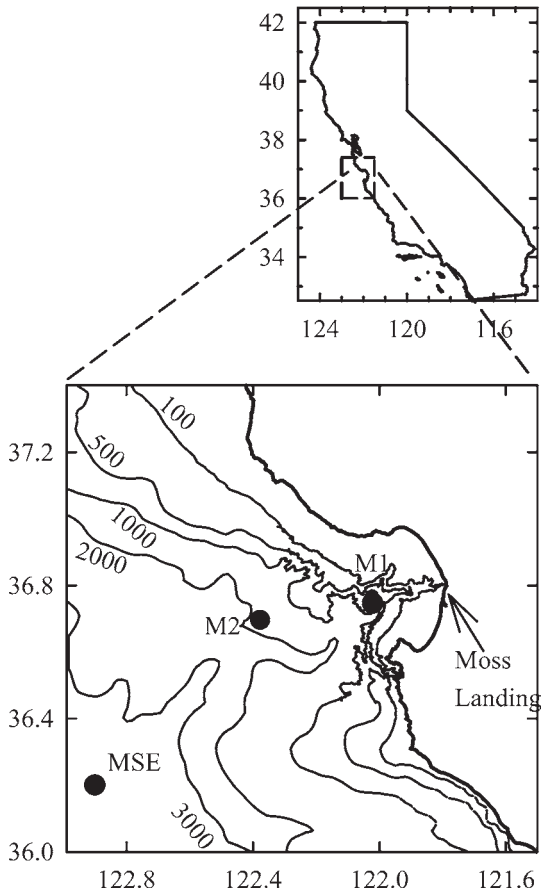

Fig. 1. M1, M2, and MSE mooring locations offshore of Monterey Bay, California. Depth contours in meters.

is a linear function of wavelength. The accuracy of nitrate concentrations calculated with the revised algorithm is significantly improved relative to the original algorithm, as shown by an extensive set of comparisons between sensor data and nitrate measurements made in the laboratory (Sakamoto et al. 2009). In relatively clear water, such as that found in Monterey Bay, and with little fouling of the sensor, which was diagnosed by observing that the baseline of the UV absorption spectrum did not drift upward, the detection limit should be near 0.5 μmol L^{-1} nitrate. However, given additional sources of uncertainty that accumulate over long-term deployments, we do not consider the results more accurate than ± 1 μmol L^{-1} nitrate. Precision of nitrate measurements is typically about 0.1 μmol L^{-1} over time periods on the order of 1 d. These metrics are generally consistent with other assessments of ISUS performance (Christensen and Melling 2009).

The pCO_2 difference between seawater (SW) and air ($\Delta pCO_2 = pCO_{2,\,SW} - pCO_{2,\,Air}$) was measured as described in Friederich et al. (1995, 2002). The $pCO_{2,\,SW}$ was estimated from ΔpCO_2 by assuming that $pCO_{2,\,Air}$ was constant at 380 μatm. Air pCO_2 was likely not constant at 380 μatm during this period. However, the data analysis discussed below focuses primarily on daily changes in chemical properties, and longer-term changes in $pCO_{2,\,Air}$ will not affect the results. Titration alkalinity (TA) was

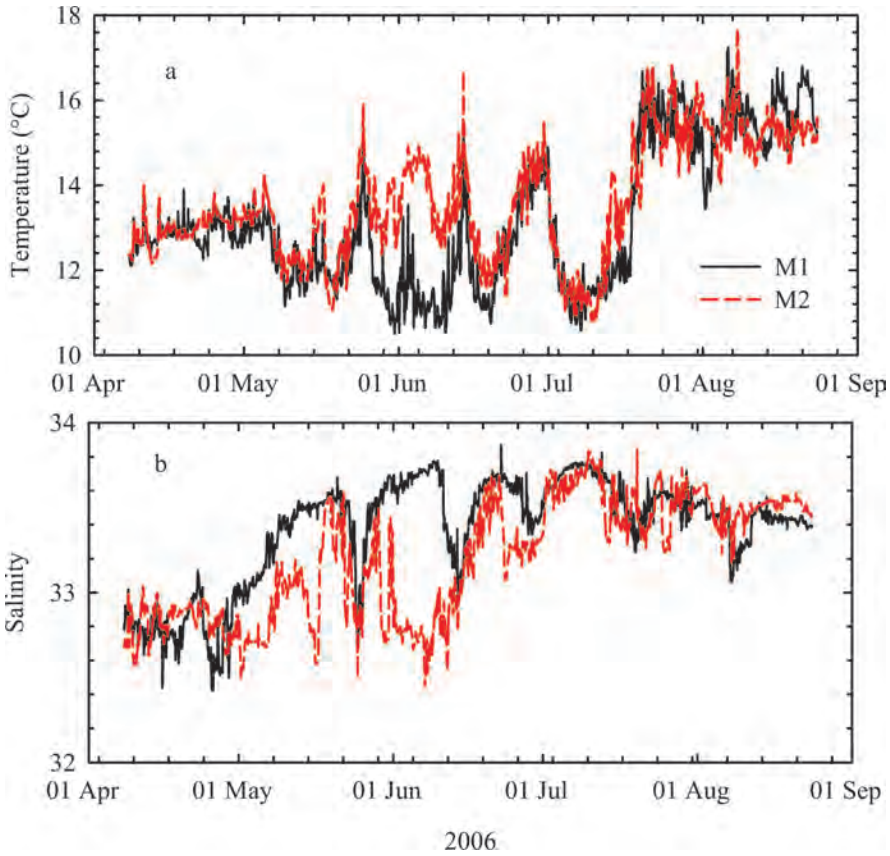

Fig. 2. (a) Temperature and (b) salinity at the M1 (black line) and M2 (dashed red line) moorings.

estimated from the observed salinity and temperature (Lee et al. 2006). TCO_2 was then calculated using the CO2SYS_MACRO_PC Excel spreadsheet program (Pierrot et al. 2006) with the observed T and S and the estimates of $pCO_{2,\,SW}$ and TA as inputs. Oxygen was measured with an Aanderaa Oxygen optode (Tengberg et al. 2006) at 1-m depth. The optode measures oxygen partial pressure and the in situ salinity and temperature were used to compute oxygen concentration using algorithms supplied by Aanderaa. The optode was protected from fouling with a copper mesh pad as suggested by the manufacturer. Chlorophyll fluorescence was measured with a WetLabs WetStar fluorometer on each mooring. Temperature and salinity were measured with SeaBird Model 37 CTD sensors.

Results

The results for temperature and salinity on the M1 and M2 moorings are shown in Fig. 2. Daily average chlorophyll and hourly values of nitrate, oxygen, and total inorganic carbon concentrations are shown in Fig. 3. Chlorophyll was binned to daily averages because of the large diurnal cycle produced by daytime fluorescence quenching (Falkowski and Kiefer 1985). In principle, nighttime values of chlorophyll fluorescence are most useful, but most samples near the moorings are collected during the day when quenching is most severe. Daily averages are used here as a compromise.

The accuracy of the chemical data may be compromised by a variety of issues, such as improper calibration, sensor fouling, or faulty assumptions made in the computation of concentrations. Shipboard observations of nitrate and oxygen provide one means to assess data accuracy (Fig. 3). Although those data are sparse, no significant drift in sensor response and accuracy within 1 μmol L^{-1} for nitrate and 5 μmol L^{-1} for oxygen is indicated, except for the M2 oxygen sensor. The M2 oxygen calibration appears to yield concentrations that are too high by 30 μmol L^{-1} (Fig. 3f), but this offset remains constant over the period considered here. The primary focus of this article is on high-frequency (daily) variations in concentration, and constant offsets in the data will not affect the main conclusions. There are no comparable shipboard observations for TCO_2, and it is conceivable that there could be high-frequency biases in those data. For example, the TCO_2 data would have a daily bias if the assumed atmospheric pCO_2 has a daily variation, perhaps due to diel variability in wind direction. One independent assessment of the TCO_2 data that can be made is comparison to values measured in the northeastern Pacific during the World Ocean Circulation Experiment (WOCE). The WOCE TCO_2 concentrations are plotted vs. nitrate in Fig. 4 along with the values estimated at M1 and M2. The WOCE data were obtained from the eWOCE electronic atlas (Schlitzer 2000) by extracting all TCO_2 and nitrate data from the upper 200 m and collected within the box

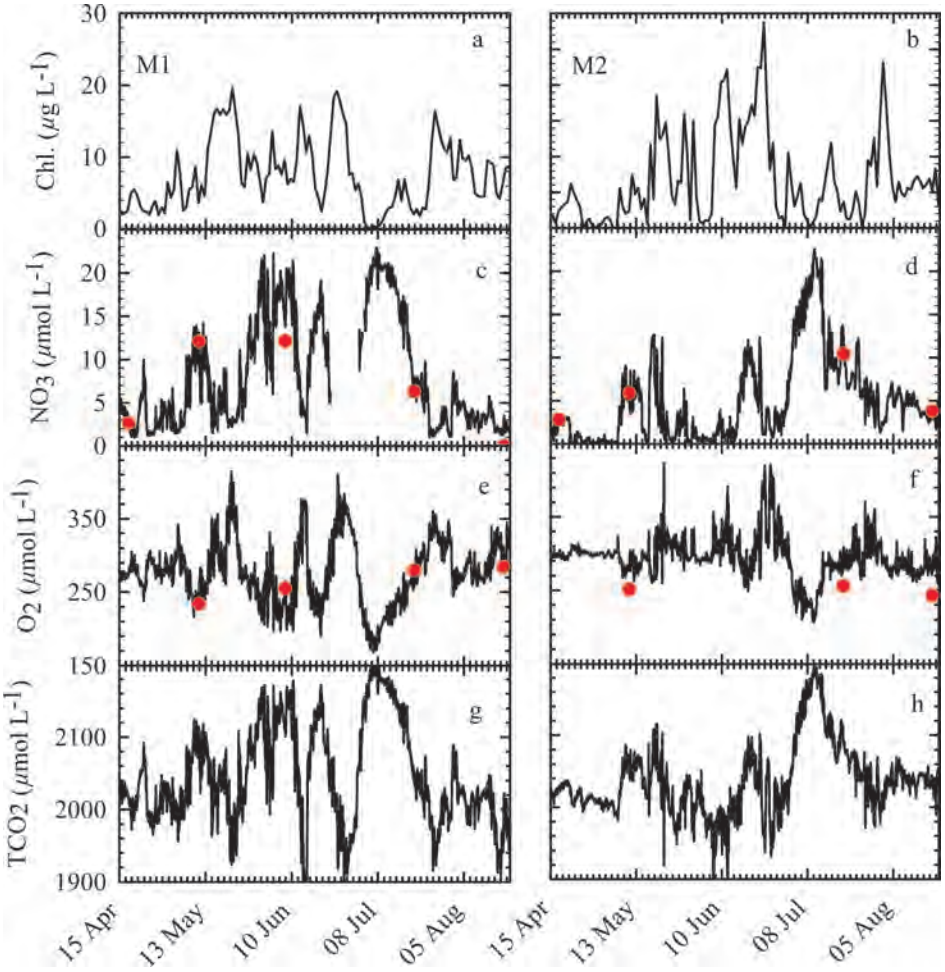

Fig. 3. Daily mean values of chlorophyll (chl) at the (a) M1 and (b) M2 moorings. Hourly values of (c, d) nitrate, (e, f) dissolved oxygen, and (g, h) TCO_2 at M1 and M2. Red dots show measured concentrations of nitrate and oxygen in samples collected near each mooring.

bounded by 30–39°N, 138–118°W. All concentrations were converted from μmol kg^{-1} to μmol L^{-1} units, and TCO_2 was normalized to a salinity of 33.4, typical of the values observed at the moorings. The standard deviation of the data about least-squares lines of TCO_2 fitted to NO_3^- for each set of data are similar (27, 22, and 20 μmol TCO_2 L^{-1} for M1, M2 and WOCE), indicating that the combined sources of variability in the mooring data are only slightly larger than in the WOCE data. As discussed below, this additional variability appears to be related to high coastal primary production. The slope of the WOCE data set is somewhat higher than at M1 and M2, which may reflect inaccuracy in the estimates of titration alkalinity used to compute TCO_2 from pCO_2 at M1 and M2. However, that should not affect conclusions regarding high-frequency process. The final assessment of the suitability of the TCO_2 data for the uses described here must come from the consistency of the results discussed next.

Discussion

Much of the temporal variability in properties seen in Figs. 2 and 3 is created by a sequence of upwelling events that bring cold, salty, nutrient-rich water to the surface. During upwelling events, the M1 mooring lies directly in the path of an upwelled plume of water that originates near Point Año Nuevo to the north of Monterey Bay (Breaker

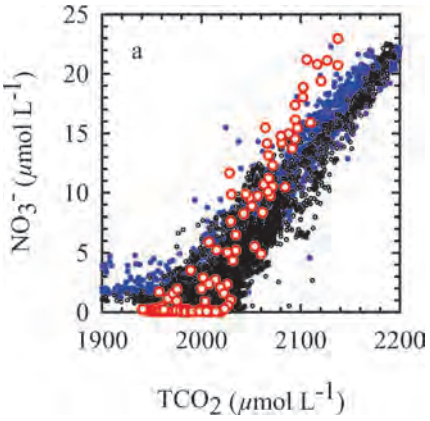

Fig. 4. Nitrate is plotted vs. TCO_2 at the M1 (black dots) and M2 (blue dots) moorings. Open red circles show near-surface values for the same parameters in the northeastern Pacific obtained during the WOCE program (Schlitzer 2000).

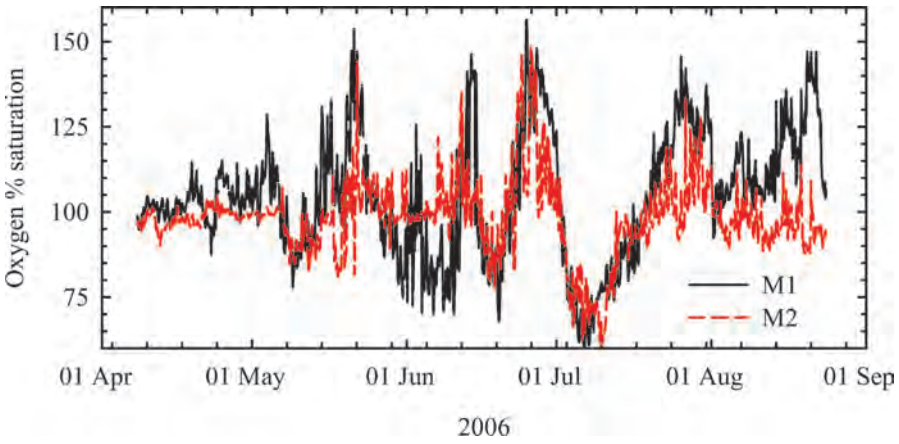

Fig. 5. Oxygen percent saturation with respect to atmospheric solubility at the M1 (black line) and M2 (dashed red line) moorings. M2 oxygen data were corrected for constant sensor offset by subtracting 30 μmol L^{-1} from each reading before computing the percent saturation.

and Broenkow 1994; Rosenfeld et al. 1994; Fitzwater et al. 2003). In strong upwelling events, the plume reaches the M2 mooring about 1 d after reaching M1. The temporal patterns in temperature at M1 and M2 are generally similar. There is one upwelling event at M1 in late May and early June that, apparently, did not reach M2, as there is no corresponding temperature or salinity signal (Fig. 2).

These upwelling events lead to large changes in chemical concentrations (Fig. 3). During these events, concentrations of nitrate, oxygen, and total inorganic carbon are highly correlated at each mooring (e.g., Fig. 4). These correlations are driven by both physical mixing or transport of waters with different properties and by in situ production or respiration of fixed organic carbon. The effects of physical and biological processes on bulk chemical concentrations are difficult to separate in this dynamic environment because both have similar signatures. Upwelled waters are enriched in nitrate and TCO_2 and depleted in oxygen as a result of respiration of organic matter. This produces chemical concentrations that are highly correlated when deep water mixes with surface waters. The same signals are produced by local uptake of nitrate and inorganic carbon and production of oxygen during daily photosynthesis and respiration cycles.

One line of evidence that points to high local rates of primary production is the high degree of oxygen saturation. The oxygen concentration reaches values well above saturation with respect to atmospheric oxygen. Percent saturation of oxygen is as high as 150% at M1 and M2 (Fig. 5). Local heating can also create supersaturation, but temperature changes of more than 18°C would be required to increase saturation by 50%. Local heating appears to change temperature by less than 5°C. The high percent saturation implies that local rates of primary production must be an important process in controlling surface oxygen concentration.

High-pass-filtered chemical concentrations—Diel cycles in nitrate concentration are regularly observed with in situ sensors (Johnson et al. 2006). These cycles are produced by nitrate uptake during daylight and resupply during the dark. The daily cycle can be used as a quantitative metric of net primary production (Johnson et al. 2006). This analysis of diel patterns involves high-pass filtering the data using a fast Fourier transform (Press et al. 1986) so that only signals with a period shorter than 33 h remain in the data set. The high-pass filter removes low-frequency changes in the data that might result from mixing of multiple water masses. In this section, the data sets that result after applying a high-pass filter to all the chemical measurements are examined.

The high-pass-filtered concentrations of nitrate, oxygen, and TCO_2 are highly correlated (Fig. 6). For example, the correlation coefficient between oxygen and TCO_2 at the M1 mooring is -0.77. Fifty-nine percent (-0.77^2) of the high-frequency variability in TCO_2 is explained by high-frequency changes in oxygen concentration. This implies that errors in the calculated TCO_2 due to high-frequency biases in titration alkalinity or atmospheric pCO_2 and that would not affect oxygen do not dominate the signals that we observe. The diel changes in nitrate are also highly correlated with TCO_2 and O_2 (Fig. 6), with nitrate amplitudes that are about one-tenth of the values observed for oxygen and TCO_2. However, the slopes of the high-pass-filtered property–property plots, which were determined from Model II linear regressions to account for errors in each variable (Laws 1997), are significantly different than the values expected from the Redfield ratio (Table 1). Non-Redfield values of the carbon-to-nitrogen ratio have been observed previously (Sambrotto et al. 1993; Kortzinger et al. 2001).

The discrepancy in the $O_2:TCO_2$ slope at both moorings, relative to the Redfield value, can likely be explained by the effects of gas exchange. A piston velocity of 2 m d^{-1} (10 cm h^{-1}) is a typical gas exchange rate constant at modest wind speeds (Wanninkhof et al. 2009). Air–sea gas exchange at this rate would remove 20–40% of the oxygen saturation anomaly on a daily basis with a

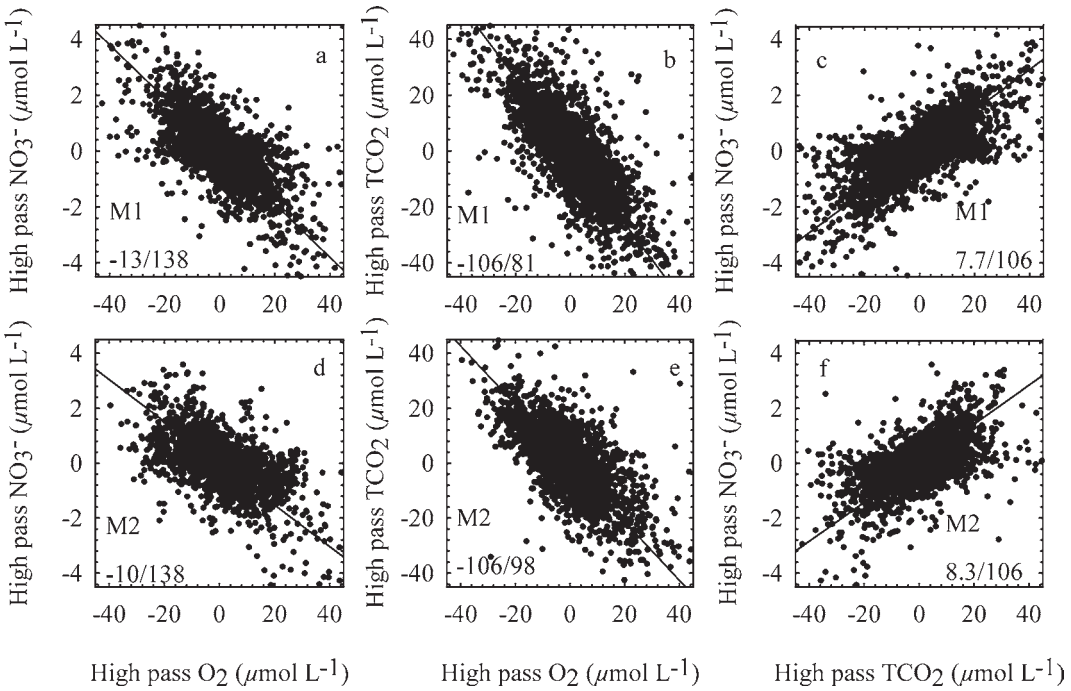

Fig. 6. High-pass-filtered concentrations of (a) nitrate and (b) TCO_2 vs. high-pass-filtered concentration of oxygen and the high-pass-filtered concentration of nitrate vs. high-pass-filtered concentration of (c) TCO_2 at the M1 mooring. Panels (d–f) are the same for the M2 mooring. Solid lines are Model II regression lines fitted to the data. Slopes of the regressions are shown in each panel.

mixed layer depth of 5–10 m, typical of the spring and summer near M1. The rate of air–sea gas exchange for TCO_2 will be about 10 times lower because of the reaction of carbon dioxide with carbonate ion, and it will be relatively unaffected by gas exchange over the same time period. As a result, gas exchange will bias the oxygen anomalies low relative to the Redfield value. This increases the slope of $TCO_2 : O_2$ graphs (Fig. 6b,e) relative to the Redfield value. If the $TCO_2 : O_2$ ratio suggested by Anderson (1995) were used rather than Redfield, the anomalies would be larger but still explainable by gas exchange processes.

To understand the reasons for the discrepancies in the observed $NO_3^- : TCO_2$ or $NO_3^- : O_2$ slopes, relative to the Redfield value, it is necessary to examine the data more closely. Fig. 7 shows one example of the unfiltered and filtered chemistry data at the M1 mooring for the period from 09 July to 16 July. The plot of the high-pass-filtered data has been scaled using the Redfield ratio (oxygen and TCO_2 anomaly ranges are the same) so that a concentration change in each property that follows Eq. 1 would span a similar vertical range. Concentration changes driven by photosynthesis are oriented up (i.e., the concentration scale for O_2 has the opposite sign as for NO_3^- and TCO_2). The end of each day in Greenwich Mean Time (GMT), which corresponds to 17:00 h local time, is near the end of daylight. There are large diel cycles, which are typified by the data in Fig. 7, with lowest nitrate and TCO_2 (highest oxygen) occurring near sunset on most days (77% of the nitrate record, 95% of the oxygen record, and 92% of the TCO_2 record). This is the result expected for a signal dominated by the effects of primary production and respiration. Cycles produced by horizontal currents would not be expected to nearly always produce minima in nitrate and TCO_2 (maxima in oxygen) near sunset (Johnson et al. 2006).

The example shown in Fig. 7 begins during a period of strong (8–10 m s^{-1}), upwelling-favorable winds that have brought cold, nitrate-rich water to the surface. Chlorophyll concentrations (Fig. 7c) are low in the freshly upwelled water. The wind began to weaken on 10 July, and chlorophyll concentrations increased rapidly. As chlorophyll increases, diel cycles develop in nitrate, oxygen, and TCO_2 that scale closely to the values expected from the Redfield ratio and that have the phasing with daylight that one would expect for a process dominated by photosyn-

Table 1. Ratios of high-pass-filtered chemical anomalies at the M1 and M2 moorings estimated from data in Fig. 6 using a Model II regression (Laws 1997). 95% confidence limits for the ratio are shown.

Ratio	Redfield	M1	M2
$NO_3^- : TCO_2$	0.15 (16 : 106)	0.073 ± 0.002 (7.7 : 106)	0.071 ± 0.002 (7.5 : 106)
$NO_3^- : O_2$	−0.12 (16 : 138)	−0.095 ± 0.003 (13 : 138)	−0.076 ± 0.002 (10 : 138)
$O_2 : TCO_2$	−1.30 (138 : 106)	−0.77 ± 0.02 (81 : 106)	−0.93 ± 0.03 (98 : 106)

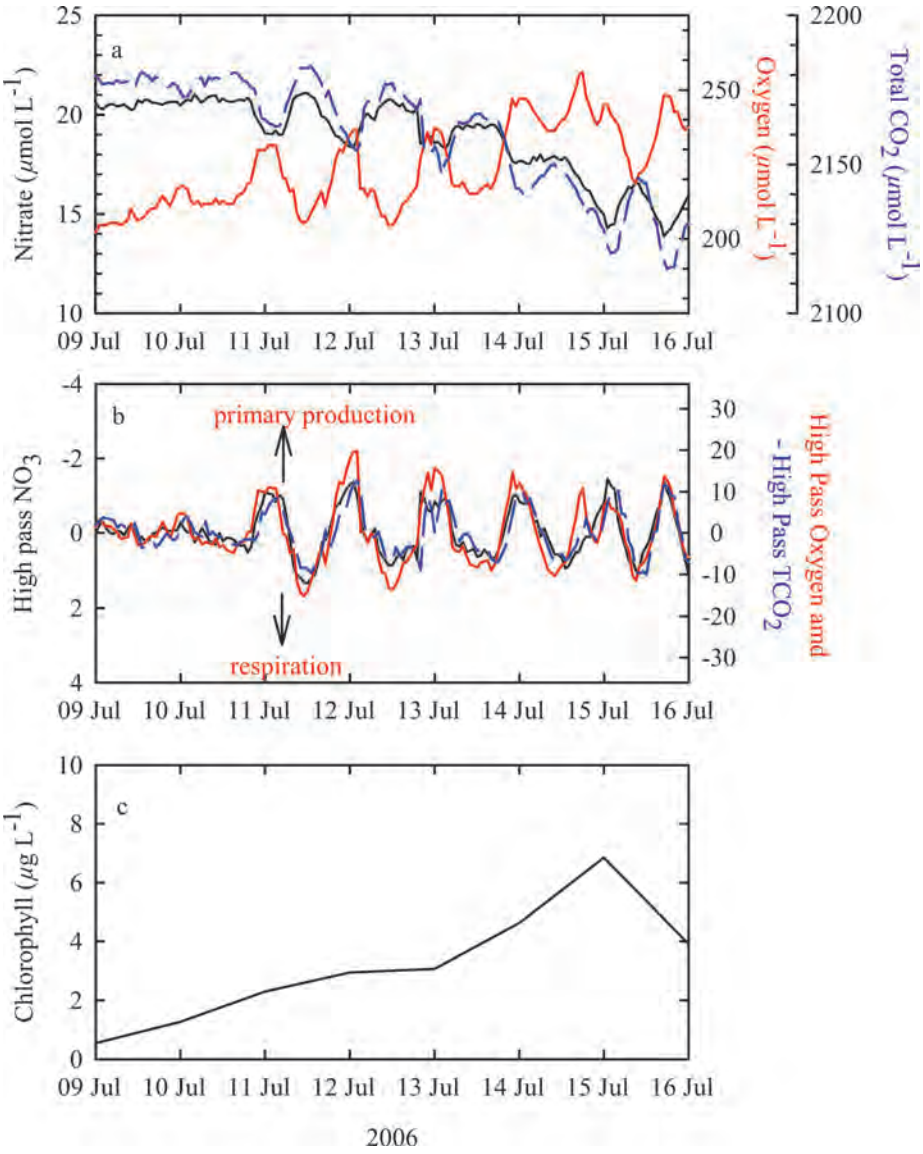

Fig. 7. (a) Concentrations of nitrate (black line), oxygen (red line), and TCO_2 (blue dashed line) from 09 July 2006 to 16 July 2006. (b) High-pass-filtered concentrations of the same properties. The axes for each filtered concentration are scaled to span a similar range when normalized to the Redfield ratio, and each scale is oriented so that changes driven by uptake during primary production are oriented up. (c) Daily average estimates of chlorophyll for the same period. Time is GMT, and local sunset is at 03:00 h.

thesis and respiration (Fig. 7b). The $NO_3^- : TCO_2$ ratio during this period is 0.12 ± 0.01 (13 : 106), somewhat closer to the Redfield value than the overall mean value of 0.073 ± 0.002 (7.7 : 106) at M1.

Figure 8 shows the chemical concentrations and their high-pass-filtered values during a subsequent period from 21 July to 30 July. Nitrate concentrations drop to low values near 1 μmol L^{-1} on 25 July and remain low for several days. Although nitrate concentration is low and its diel cycle is very small after 25 July, the diel cycles of TCO_2 and oxygen continue with large amplitudes. The large diel cycles in both TCO_2 and oxygen are unlikely to be the result of sensor fouling, as the two systems are completely independent. The low concentration values returned by the nitrate sensor are consistent with discrete samples throughout the deployment. The $NO_3^- : TCO_2$ ratio is 0.021 ± 0.007 (2.2 : 106) for 25–28 July and 0.076 ± 0.008 (8 : 106) for the period 21–30 July. There is nearly complete decoupling of nitrate from the carbon and oxygen cycles for 3 d, and the mean $NO_3^- : TCO_2$ ratio for the entire period is about half the Redfield value. Decoupling of nitrate from oxygen and carbon cycling, defined as a day when the nitrate amplitude is less than one-third of the mean amplitude of the O_2 and TCO_2 cycles on the same day (all amplitudes in carbon units), occurs about 30% of the time at M1 and M2. This leads to the low value of the $NO_3^- : TCO_2$ ratio for the entire data set. Modest increases in wind speed from a mean of 2 m s^{-1} over 18–23 July to

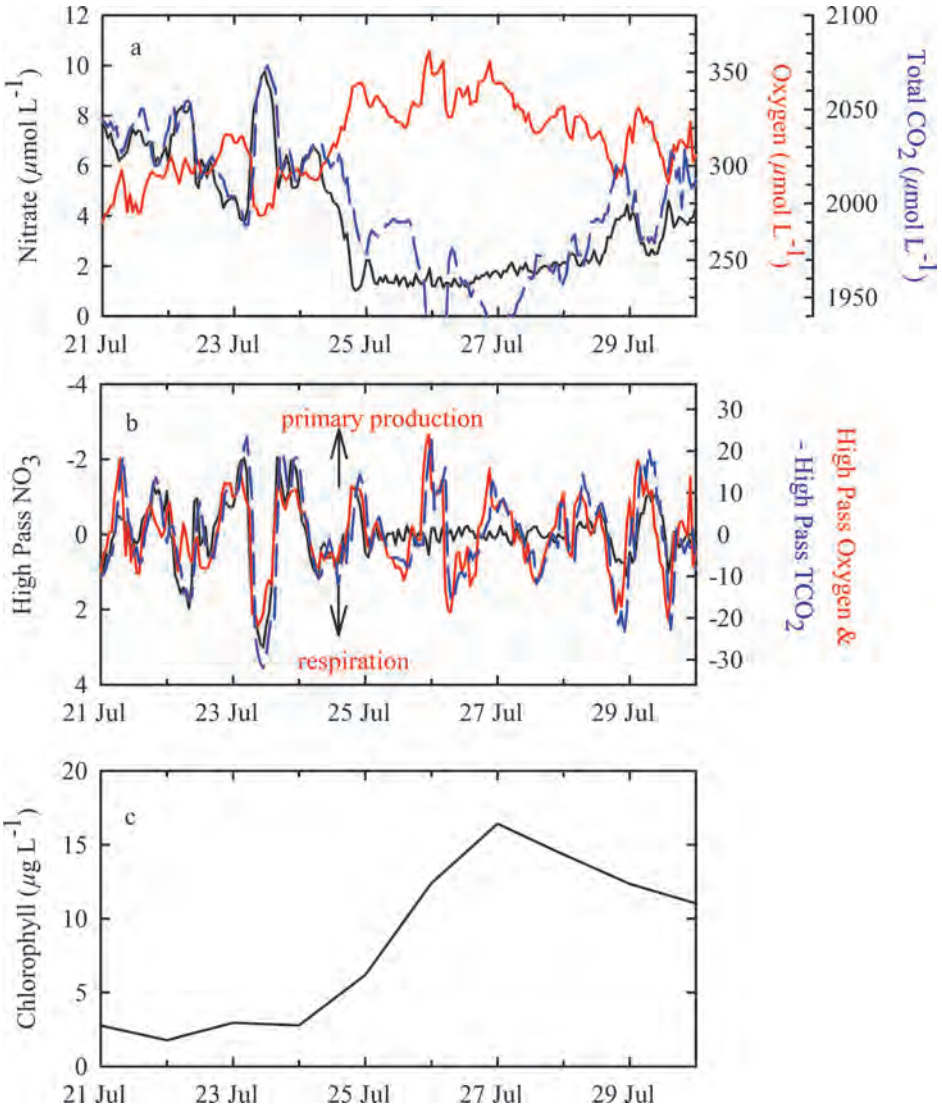

Fig. 8. As in Fig. 7 for the period 21 July 2006–30 July 2006.

5 m s^{-1} on 24 July lead to an increase in nitrate concentration a few days later. There is a resumption in diel nitrate cycles that match the TCO_2 and O_2 amplitudes by 29 July (Fig. 8). This would indicate that the well-developed bloom, with chlorophyll concentrations that exceed 10 μg L^{-1} (Fig. 8c), can rapidly switch back to using surface nitrate as a fixed nitrogen source at Redfield ratios. Again, the phasing of the diel cycles with extreme values at sunset matches the result one would expect for processes dominated by photosynthesis and respiration. Changing C : N ratios during the evolution of a bloom have been observed in other areas of the ocean (Sambrotto et al. 1993; Kortzinger et al. 2001). The results presented here are unique, however, as they show that shifts between high and low values of the C : N uptake ratio can occur in a matter of a few days.

The concentration of chlorophyll increases and TCO_2 decreases during the period in July with low nitrate (Fig. 8a,c), indicating that there has been net production of organic matter. There are multiple reasons why nitrate might be decoupled from the oxygen and TCO_2 cycles while organic carbon is produced. Other studies (Sambrotto et al. 1993) suggest that nitrate is decoupled from carbon cycling because nitrate is recycled preferentially in the surface. Sources of fixed nitrogen other than nitrate, such as ammonia or urea, might also fuel production of organic matter. Ammonium concentrations are observed to reach values as high as 2 μmol L^{-1} at the base of the euphotic zone in Monterey Bay (Bronk and Ward 1999; J. Plant pers. comm.), although values are more typically near 0.1 μmol L^{-1}. The diel TCO_2 and O_2 cycles on 25–28 July (Fig. 8) would require a fixed nitrogen supply near 3 μmol L^{-1} to remain in Redfield balance. The highest ammonium concentrations that are typically observed (Bronk and Ward 1999) might just be sufficient to meet this demand if the ammonium pool is depleted each day. Alternatively, a phytoplankton population consisting of dinoflagellates might be capable of migrating vertically to the nitracline to acquire nitrate and then return to the surface where photosynthesis takes place. Large dinofla-

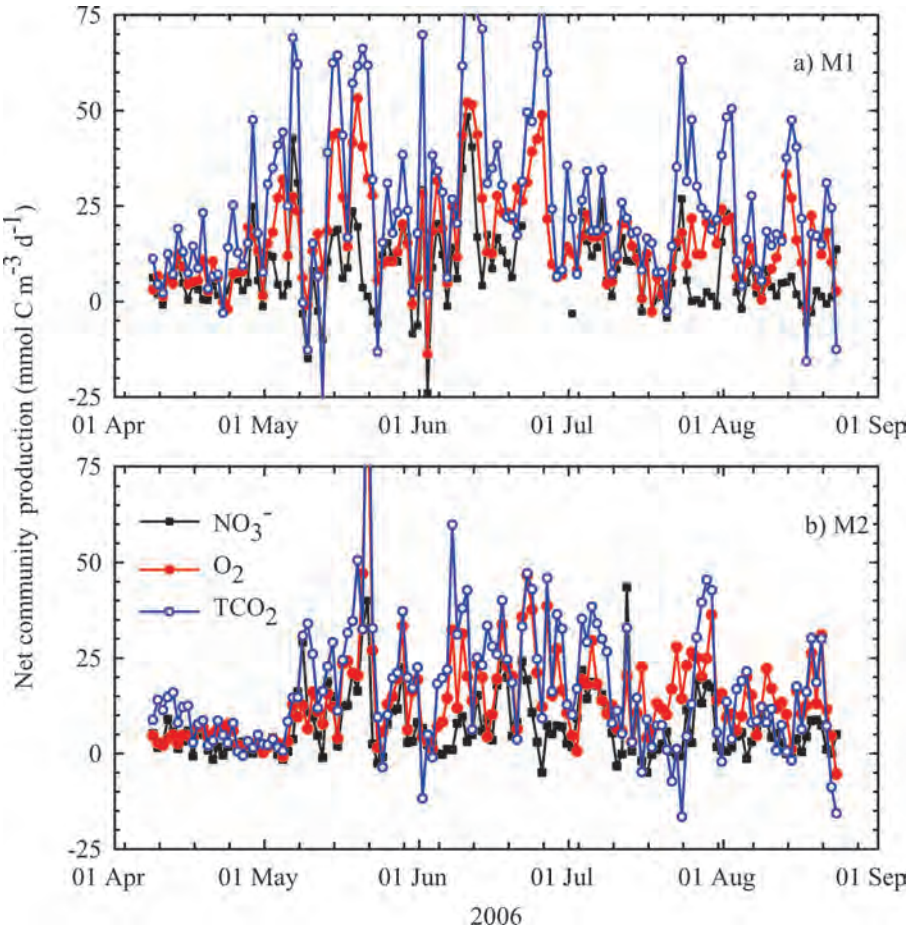

Fig. 9. Diel amplitude of the high-pass-filtered nitrate (black line), oxygen (red line), and TCO_2 (blue line) at the (a) M1 mooring and (b) M2 mooring.

gellate blooms periodically dominate in Monterey Bay, and they are observed to migrate to the nitracline (Ryan et al. 2009). These two processes cannot be resolved with the data that are available, but it would certainly be feasible to instrument moorings to put further constraints on these processes. For example, it is now possible to measure dissolved ammonia on moorings in a nearly routine manner (Plant et al. 2009). Deeper chlorophyll fluorometers could detect vertical migration. Until such measurements are made, it is not possible to determine unequivocally whether organic matter is produced with unusual carbon-to-nitrogen ratios or if the ratios are in Redfield balance, but we do not measure all the nitrogen sources. The data in Fig. 8 around 29 July indicate that the changes occur rapidly.

Biomass production—Daily estimates of net community production of organic matter were calculated from the amplitude of the high-pass-filtered concentrations. To calculate the amplitude, the minimum values of high-pass-filtered nitrate and TCO_2 (maximum for oxygen) were found each day for the period from 22:00 h to 03:00 h GMT (15:00–20:00 h Pacific Daylight Time [PDT]), and the mean concentration for the 3-h period centered on that time was calculated. Maximum values (minimum for oxygen) were found each day between 11:00 h and 16:00 h GMT (04:00–09:00 h PDT), and the mean concentration for the 3-h period centered on that time was again calculated. The diel amplitude due to primary production was set as the difference of these two values for each chemical. These diel amplitudes for nitrate and oxygen were then converted to carbon units using the Redfield ratio (Eq. 1). The results are shown in Fig. 9 for M1 and M2.

Each of the daily amplitudes of the high-pass-filtered nitrate, oxygen, and TCO_2 concentrations is an independent estimate of the net production of organic matter (Johnson et al. 2006). TCO_2- and O_2-based production values are often larger than the nitrate-based production estimates (Fig. 9). There is also one example (M2, mid- to late July; Fig. 9) where oxygen amplitude is high and the carbon and nitrate amplitudes are much lower. This may reflect fouling of the oxygen sensor, although it began returning values consistent with its early performance without any cleaning. Alternatively, it reflects a period where the TCO_2 concentration estimates are inaccurate because of assumptions about atmospheric pCO_2 or titration alkalinity. Such periods with potentially large biases in the TCO_2 seem to be relatively rare, however, because there is generally good agreement between the high-pass-filtered TCO_2 and the oxygen.

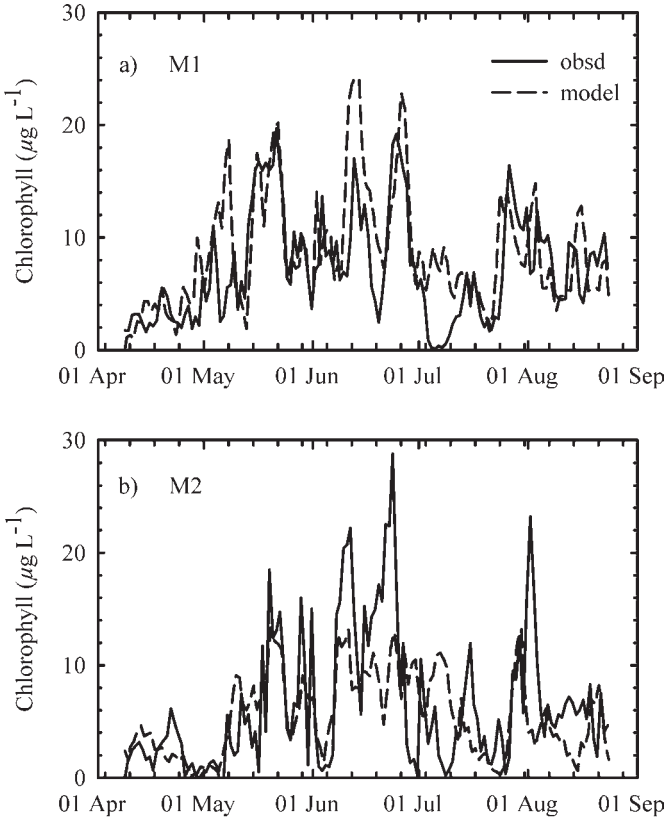

Fig. 10. Observed chlorophyll concentrations (solid lines) and values computed from Eq. 2 using net community production values estimated from the TCO_2 diel amplitude (dashed lines) are shown for the (a) M1 mooring and the (b) M2 mooring. A single high value of the TCO_2 diel amplitude at M2, which was observed on 21 May 2006 (128 mmol C m^{-3} d^{-1}) and which is off scale in Fig. 9, was replaced by the average of the two adjacent values for the model calculations.

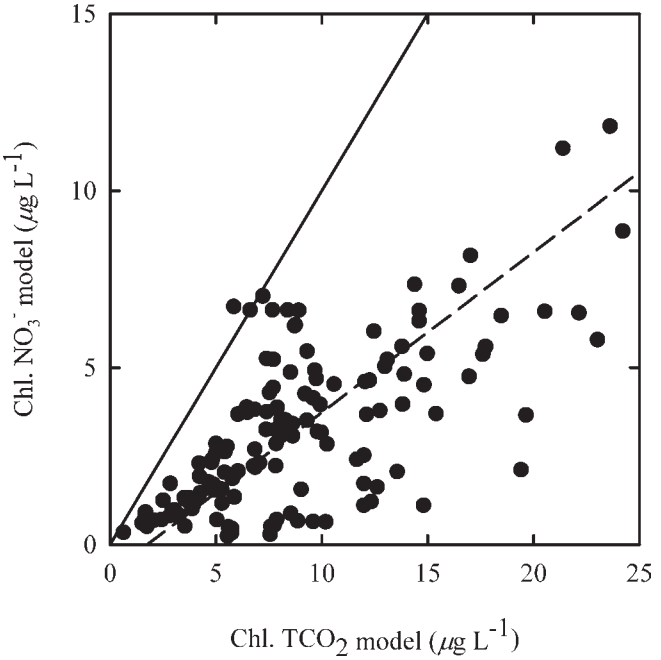

Fig. 11. Chlorophyll computed from Eq. 2 using diel amplitudes derived from nitrate observations are plotted vs. chlorophyll computed from Eq. 2 using TCO_2 diel amplitudes. The dashed line is a Model II regression with slope 0.45 ± 0.06 (95% confidence interval). The solid line has slope 1.

The daily estimates of new production can be used to predict the accumulation of biomass using the following equation (Johnson et al. 2006):

$$B_t = B_{t-1} + \Delta_t \times NCP - \Delta_t \times L \times B_{t-1} \quad (2)$$

where B is biomass in carbon units; NCP is the daily estimate of net community production of carbon derived from the diel amplitude of nitrate, oxygen, or TCO_2 measurements (Fig. 9); Δ_t is a 1-h time step; and L is the rate constant for loss of biomass due to all factors, including grazing, sinking, and removal by horizontal advection. The amplitude of the nitrate diel cycle is a reflection of net production that incorporates dissolved nitrate from surface waters, while the amplitudes of oxygen and TCO_2 would reflect production from all fixed nitrogen sources. Integration of Eq. 2 was begun with an initial biomass value of zero.

The biomass values calculated using NCP derived from the TCO_2 concentrations are shown in Fig. 10 for M1 and M2. Carbon biomass was converted to chlorophyll units using a constant C : chlorophyll ratio (by weight) of 60 (Johnson et al. 2006). L is not constrained directly by the chemical observations. It was, therefore, adjusted by comparing the predicted chlorophyll with the values observed at each mooring and minimizing the sum of the squared errors. A value of 0.6 d^{-1} is near the optimum at both M1 and M2, and that value has been used to compute the predicted chlorophyll concentrations shown in Fig. 10. The estimates of chlorophyll that are derived from NCP values based on the diel cycle of TCO_2 are significantly correlated with the observed, daily mean values of chlorophyll with an $R^2 = 0.45$ at M1 and $R^2 = 0.25$ at M2 ($p < 0.0001$ in each case). The predicted chlorophyll values capture nearly all the major bloom cycles seen at both moorings (Fig. 10). These results demonstrate that it is possible to use in situ chemical observations to determine how much carbon is produced each day and, with a single adjustable parameter that relates to biomass loss, to also predict the temporal course of biomass standing stocks over periods of multiple months.

Similar results for biomass standing stocks are found using the high-pass-filtered data for dissolved oxygen when it is converted to carbon units using the Redfield ratio. For example, the R^2 between chlorophyll modeled with productivity based on oxygen daily amplitude and observed values is 0.48 at M1. However, the time course of biomass predicted using high-pass-filtered nitrate concentrations is somewhat different for the period of this study. The modeled chlorophyll values determined using NCP derived from TCO_2 and nitrate (after conversion to carbon units with the Redfield ratio) are plotted vs. each other in Fig. 11. While the two values are highly correlated ($R^2 =$

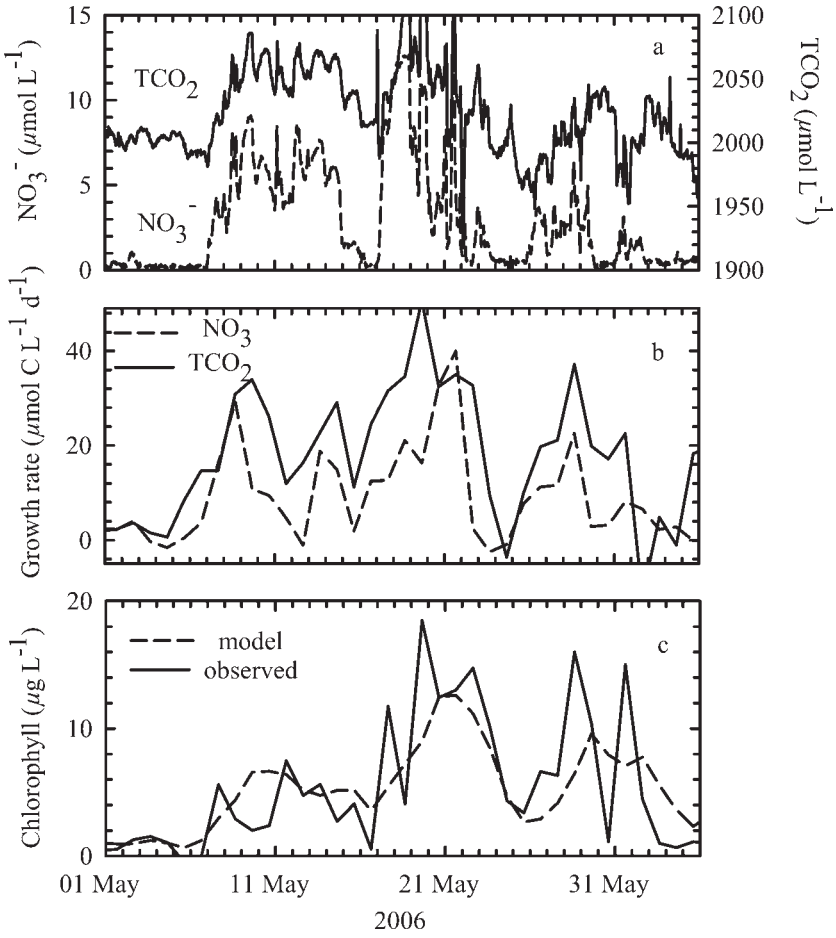

Fig. 12. (a) Nitrate (dashed line) and TCO_2 (solid line) concentrations observed at the M2 mooring from 01 May 2006 to 05 June 2006. (b) Diel amplitudes of nitrate, after conversion to carbon units using the Redfield ratio (dashed line) and TCO_2 (solid line), are shown for the same time period. (c) Observed daily mean chlorophyll values (solid line) and values computed from Eq. 2 using the diel amplitudes derived from TCO_2 (dashed line) are shown for the same time period.

0.47), the slope of a line fitted to all the data is 0.45 rather than the expected value of 1. If the value of L is optimized using growth rates based on nitrate, the best-fit value is 0.33 d^{-1} rather than 0.6 d^{-1} when TCO_2 daily amplitudes are used. The diel cycles based on nitrate concentrations predict, on average, only about half the biomass accumulation predicted from TCO_2 cycles when the same value of L is used. This occurs because, as noted above, on about 30% of the days, the NCP value estimated from the diel nitrate amplitude is less than one-third of the value estimated from TCO_2 or O_2. Presumably, the remainder of the biomass accumulation that is observed or that is modeled using NCP derived from daily cycles of TCO_2 and O_2 is derived from fixed nitrogen sources other than the nitrate that is found in surface waters. These sources might include ammonium or vertical migration to obtain nitrate at greater depths.

Phytoplankton net community production appears to be fueled by nitrate early in upwelling periods, and then other sources, as discussed above, become important. Figure 12 shows the sequence of events during an upwelling period in May 2006 at the M2 mooring. Nitrate concentrations increase from near-zero values to 12 μmol L^{-1} in two main pulses. TCO_2 increases in parallel with nitrate, and it clearly shows diel cycles with minima at sunset on most days. Net community production rates based on diel amplitudes of TCO_2 and NO_3^- (Fig. 12b) increase within the nutrient-rich, upwelled water from near-zero values before onset of the upwelling event. As these growth rates increase, both the modeled and the observed chlorophyll concentrations increase at similar rates. Observed chlorophyll and values modeled using TCO_2 diel cycles continue to increase, while dissolved nitrate is present to fuel growth. The chlorophyll concentration declines in late May, as nitrate is depleted. The growth rates based on nitrate track the values based on TCO_2 near the beginning of the upwelling period. However, as biomass increases, the growth rates based on TCO_2 exceed those based on nitrate. Either the phytoplankton are growing with C : N ratios that are nearly double the Redfield value or recycled nitrogen in the form of ammonia begins to serve as a significant N source as biomass.

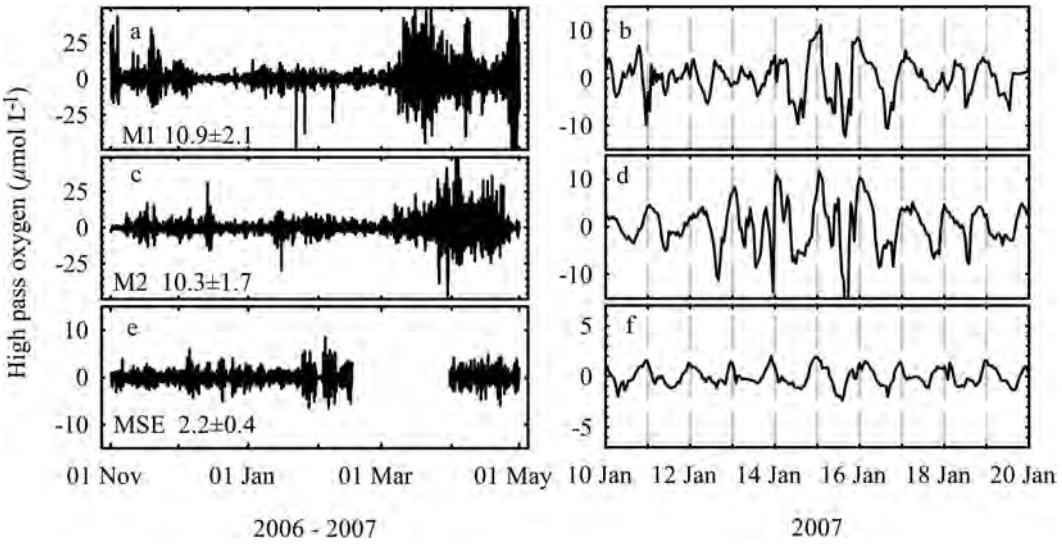

Fig. 13. High-pass-filtered oxygen concentrations from (a) 01 November 2006 to 10 May 2007 and (b) 10 January 2007 to 20 January 2007 at the M1 mooring. Panels (c, d) are the same at the M2 mooring. Panels (e, f) are the same at the MSE mooring. The mean and 95% confidence intervals are shown in panels (a, c, e).

Limits of detection—In order to assess the lower limits of production at which diel chemical cycles can be detected, oxygen sensor data from the MSE mooring, which was deployed at 115 km off the coast, is considered. High-pass-filtered oxygen data from M1, M2, and MSE from November 2006 to May 2007 are shown in Fig. 13a, c, and e. One large gap in the MSE data occurred when the sensor fouled, diagnosed as a rapid increase in diel amplitude, followed by a drop to near-zero oxygen concentration. After the sensor was cleaned and the antifouling copper mesh was replaced, the sensor began to return measurements similar to values observed before the fouling event. Clear diel cycles with maxima near the end of daylight are seen at the MSE mooring, as well as at M1 and M2, throughout this period (Fig. 13b,d,f). The mean values of the diel amplitude for the November–May period are shown in Fig. 13a, c, and e. The amplitude at the MSE mooring (2.2 ± 0.4 mmol O_2 m^{-3} d^{-1}, 95% CI) is a factor of 5 lower than at M1 and M2, and it is easily resolved during this period. A lower limit to reliable detection is probably around 0.5–1 mmol O_2 m^{-3} d^{-1}. The values at the MSE mooring, which was 115 km offshore, approach the amplitudes that one might expect in oligotrophic waters, based on light and dark bottle incubations (Williams et al. 2004).

In conclusion, the results shown here demonstrate that the daily cycles of inorganic carbon, oxygen, and nitrate are often closely coupled in ratios near those expected from Redfield (Eq. 1). However, there is also significant decoupling of the observed parameters on about 30% of the days. This is particularly true for the C : N ratio. Because only nitrate was sensed, which is one of many possible forms of fixed nitrogen, this decoupling does not demonstrate that organic matter is produced with distinctly non-Redfieldian composition. Rather, it most likely indicates that, even in dynamic, coastal upwelling ecosystems, nitrate present in surface waters is not always the dominant fixed nitrogen source for phytoplankton. In Monterey Bay, only about half the required nitrogen appears to be supplied directly from surface waters during the time of this study.

Acknowledgments

Efforts of Gernot Friederich, Francisco Chavez, Luke Coletti, Carole Sakamoto, Mike Kelley, Paul Coenen, and Mark Chaffey to support sensor deployments on the M1, M2, and MSE moorings are greatly appreciated. This work was supported by the David and Lucile Packard Foundation. Comments by Mike DeGrandpre and an anonymous reviewer greatly improved the manuscript, and their advice is gratefully acknowledged.

References

Anderson, L. A. 1995. On the hydrogen and oxygen content of marine phytoplankton. Deep-Sea Res. I **42:** 1675–1680.

———, and J. L. Sarmiento. 1994. Redfield ratios of remineralization determined by nutrient data analysis. Glob. Biogeochem. Cycles **8:** 65–80.

Breaker, L. C., and W. W. Broenkow. 1994. The circulation of Monterey Bay and related processes. Oceanogr. Mar. Biol. Annu. Rev. **32:** 1–64.

Broecker, W. S. 1974. "NO" a conservative water-mass tracer. Earth Planet. Sci. Lett. **23:** 100–107.

Bronk, D. A., and B. B. Ward. 1999. Gross and net nitrogen uptake and DON release in the euphotic zone of Monterey Bay, California. Limnol. Oceanogr. **44:** 573–585.

Chavez, F. P., J. T. Pennington, R. Herlien, H. Jannasch, G. Thurmond, and G. E. Friederich. 1997. Moorings and drifters for real-time interdisciplinary oceanography. J. Atmos. Ocean. Technol. **14:** 1199–1211.

Christensen, J. P., and H. Melling. 2009. Correcting nitrate profiles measured by the in situ ultraviolet spectrophotometer in Arctic Ocean waters. Open Oceanogr. J. **3:** 59–66.

Degrandpre, M. D., A. Kortzinger, U. Send, D. W. R. Wallance, and R. G. J. Bellerby. 2006. Uptake and sequestration of atmospheric CO_2 in the Labrador Sea deep convection region. Geophys. Res. Lett. **33:** L21S03, doi:10.1029/2006GL026881.

DEUTSCH, C., J. L. SARMIENTO, D. M. SIGMAN, N. GRUBER, AND J. P. DUNNE. 2007. Spatial coupling of nitrogen inputs and losses in the ocean. Nature **445:** 163–167.

FALKOWSKI, P. G. 2000. Rationalizing elemental ratios in unicellular algae. J. Phycol. **36:** 3–6.

———, AND D. A. KIEFER. 1985. Chlorophyll *a* fluorescence in phytoplankton: Relationship to photosynthesis and biomass. J. Plankton Res. **7:** 715–731.

FITZWATER, S. E., AND OTHERS. 2003. Iron, nutrient and phytoplankton biomass relationships in upwelled waters of the California coastal system. Cont. Shelf Res. **23:** 1523–1544.

FRIEDERICH, G. E., P. G. BREWER, R. HERLIEN, AND F. P. CHAVEZ. 1995. Measurements of sea surface partial pressure of CO_2 from a moored buoy. Deep-Sea Res. I **42:** 1175–1186.

———, P. M. WALZ, M. G. BURCZYNSKI, AND F. P. CHAVEZ. 2002. Inorganic carbon in the central California upwelling system during the 1997–1999 El Nino–La Nina event. Prog. Oceanogr. **54:** 185–203.

GRUBER, N., AND J. L. SARMIENTO. 1997. Global patterns of marine nitrogen fixation and denitrification. Glob. Biogeochem. Cycles **11:** 235–266.

JOHNSON, K. S., AND L. J. COLETTI. 2002. In situ ultraviolet spectrophotometry for high resolution and long term monitoring of nitrate, bromide and bisulfide in the ocean. Deep-Sea Res. I **49:** 1291–1305.

———, ———, AND F. P. CHAVEZ. 2006. Diel nitrate cycles observed with in situ sensors predict monthly and annual new production. Deep-Sea Res. I **53:** 561–573.

———, J. A. NEEDOBA, S. C. RISER, AND W. J. SHOWERS. 2007. Chemical sensor networks for the aquatic environment. Chem. Rev. **107:** 623–640.

KARL, D. M., AND OTHERS. 2001. Ecological nitrogen-to-phosphorous stoichiometry at station ALOHA. Deep-Sea Res. II **48:** 1529–1566.

KELLER, K., R. D. SLATER, M. BENDER, AND R. M. KEY. 2002. Possible biological or physical explanations for decadal scale trends in North Pacific nutrient concentrations and oxygen utilization. Deep-Sea Res. II **49:** 345–362.

KLAUSMEIER, C. A., E. LICHMAN, T. DAUFRESNE, AND S. A. LEVIN. 2004. Optimal nitrogen-to-phosphorous stoichiometry of phytoplankton. Nature **429:** 171–174.

KORTZINGER, A., W. KOEVE, P. KAHLER, AND L. MINTROP. 2001. C : N ratios in the mixed layer during the productive season in the northeast Atlantic Ocean. Deep Sea Res. I **48:** 661–688.

———, U. SEND, D. W. R. WALLACE, J. KARSTENSEN, AND M. DEGRANDPRE. 2008*a*. Seasonal cycle of O_2 and pCO_2 in the central Labrador Sea: Atmospheric, biological, and physical implications. Global Biogeochem. Cycles **22:** GB1014, doi:10.1029/2007GB003029.

———, AND OTHERS. 2008*b*. The seasonal pCO_2 cycle at 49°N/16.5°W in the northeastern Atlantic Ocean and what it tells us about biological productivity. J. Geophys. Res. **113:** C04020, doi:10.1029/2007JC004347.

LAWS, E. A. 1997. Mathematical methods for oceanographers: An introduction. Wiley-Interscience.

LEE, K., AND OTHERS. 2006. Global relationships of total alkalinity with salinity and temperature in surface waters of the world's oceans. Geophys. Res. Lett. **33:** L19605, doi:10.1029/2006GL027207.

LENTON, T. M., AND A. J. WATSON. 2000. Redfield revisited 1. Regulation of nitrate, phosphate, and oxygen in the ocean. Global Biogeochem. Cycles **14:** 225–248.

LI, Y.-H., AND T.-H. PENG. 2002. Latitudinal change of remineralization ratios in the oceans and its implication for nutrient cycles. Global Biogeochem. Cycles **16:** 1130, doi:10.1029/2001GB001828.

MORRIS, A. W., AND J. P. RILEY. 1966. The bromide/chlorinity and sulphate/chlorinity ratio in sea water. Deep-Sea Res. **13:** 699–705.

ODUM, H. T. 1956. Primary production in flowing waters. Limnol. Oceanogr. **1:** 102–117.

PAHLOW, M., AND U. RIEBESELL. 2000. Temporal trends in deep ocean Redfield ratios. Science **287:** 831–833.

PIERROT, D., E. LEWIS, AND D. W. R. WALLACE. 2006. MS Excel program developed for CO_2 system calculations. ORNL/CDIAC-105. Carbon Dioxide Information Analysis Center, Oak Ridge National Laboratory, U.S. Department of Energy, Oak Ridge, Tennessee.

PLANT, J. N., K. S. JOHNSON, J. A. NEEDOBA, AND L. J. COLETTI. 2009. NH4-Digiscan: An in situ and laboratory ammonium analyzer for estuarine, coastal and shelf waters. Limnol. Oceanogr.: Methods **7:** 144–156.

PRESS, W. H., B. P. FLANNERY, S. A. TEUKOLSKY, AND W. T. VETTERLING. 1986. Numerical recipes. Cambridge University Press.

REDFIELD, A. C. 1934. On the proportions of organic derivatives in sea water and their relation to the composition of plankton, p. 177–192. *In* R. J. Daniel [ed.], James Johnstone Memorial Volume. University Press of Liverpool.

ROSENFELD, L. K., F. B. SCHWING, N. GARFIELD, AND D. E. TRACY. 1994. Bifurcated flow from an upwelling center: A cold water source for Monterey Bay. Cont. Shelf Res. **14:** 931–964.

RYAN, J. P., A. M. FISCHER, R. M. KUDELA, J. F. R. GOWER, S. A. KING, R. MARIN, AND F. P. CHAVEZ. 2009. Influences of upwelling and downwelling winds on red tide bloom dynamics in Monterey Bay, California. Cont. Shelf Res. **29:** 785–795.

SAKAMOTO, C. M., K. S. JOHNSON, AND L. J. COLETTI. 2009. An improved algorithm for the computation of nitrate concentrations in seawater using an in situ ultraviolet spectrophotometer. Limnol. Oceanogr.: Methods **7:** 132–143.

SAMBROTTO, R. N., AND OTHERS. 1993. Elevated consumption of carbon relative to nitrogen in the surface ocean. Nature **363:** 248–250.

SCHLITZER, R. 2000. Electronic atlas of WOCE hydrographic and tracer data now available. Eos Trans. Am. Geophys. Union **81:** 45.

TENGBERG, A., AND OTHERS. 2006. Evaluation of a lifetime-based optode to measure oxygen in aquatic systems. Limnol. Oceanogr.: Methods **4:** 7–17.

TYRRELL, T., AND M. I. LUCAS. 2002. Geochemical evidence of denitrification in the Benguela upwelling system. Cont. Shelf Res. **22:** 2497–2511.

WANNINHKOF, R., W. E. ASHER, D. T. HO, C. S. SWEENEY, AND W. R. MCGILLIS. 2009. Advances in quantifying air-sea gas exchange and environmental forcing. Annu. Rev. Mar. Sci. **1:** 213–244.

WILLIAMS, P. J. LE B., P. J. MORRIS, AND D. M. KARL. 2004. Net community production and metabolic balance at the oligotrophic ocean site, station ALOHA. Deep-Sea Res. I **51:** 1563–1578.

YATES, K. K., C. DUFORE, N. SMILEY, C. JACKSON, AND R. B. HALLEY. 2007. Diurnal variation of oxygen and carbonate system parameters in Tampa Bay and Florida Bay. Mar. Chem. **104:** 110–124.

Associate editor: Robert R. Bidigare

Received: 13 May 2009
Accepted: 04 October 2009
Amended: 01 December 2009